nature climate change

LETTERS

PUBLISHED ONLINE: 16 FEBRUARY 2015 | DOI: 10.1038/NCLIMATE2530

Contemporary white-band disease in Caribbean corals driven by climate change

C. J. Randall* and R. van Woesik

Over the past 40 years, two of the dominant reef-building corals in the Caribbean, *Acropora palmata* and *Acropora cervicornis*, have experienced unprecedented declines[1,2]. That loss has been largely attributed to a syndrome commonly referred to as white-band disease[1,3]. Climate change-driven increases in sea surface temperature (SST) have been linked to several coral diseases[4,5], yet, despite decades of research, the attribution of white-band disease to climate change remains unknown. Here we hindcasted the potential relationship between recent ocean warming and outbreaks of white-band disease on acroporid corals. We quantified eight SST metrics, including rates of change in SST and contemporary thermal anomalies, and compared them with records of white-band disease on *A. palmata* and *A. cervicornis* from 473 sites across the Caribbean, surveyed from 1997 to 2004. The results of our models suggest that decades-long climate-driven changes in SST, increases in thermal minima, and the breach of thermal maxima have all played significant roles in the spread of white-band disease. We conclude that white-band disease has been strongly coupled with thermal stresses associated with climate change, which has contributed to the regional decline of these once-dominant reef-building corals.

Acropora palmata and *Acropora cervicornis* emerged as dominant framework-building corals in the Caribbean in the middle of the Pliocene epoch, some 3.5 million years ago[6], when ocean temperatures were cooling[7]. Since then, these two coral species have been among the most dominant Caribbean reef builders[2]. Yet over the past 40 years their populations have declined by >90% in many localities throughout the Caribbean[1,2]. This decline has been partially attributed to outbreaks of a syndrome known as white-band disease[1,3] (Fig. 1). Consequently, *A. palmata* and *A. cervicornis* are now listed as critically endangered on the International Union for Conservation of Nature (IUCN) Red List of Threatened Species[8], and are listed as threatened under the US Endangered Species Act of 1973 (ref. 9). With the exception of a few localized areas, the recovery of *Acropora* in the Caribbean has been uncommon, and the disease persists on reefs that still support *Acropora* populations[10] (Supplementary Fig. 1).

Despite the severity of the syndrome, and its early detection in the 1970s (ref. 3), the aetiology of white-band disease remains poorly understood. Molecular studies have identified significant differences in the microbial communities on tissues with and without macroscopic signs of white-band disease, suggesting that the disease may be caused by bacterial pathogens[11,12]. Drug-treatment experiments using ampicillin and paromomycin were effective at arresting white-band disease on *A. cervicornis*, also suggesting that the causative agent may be one or more bacteria[13]. Similarly, a field experiment in the US Virgin Islands identified significant spatial clusters of *A. palmata* colonies with white-band disease, suggesting that a contagious pathogen was being locally transmitted through the population[14]. In combination, many of

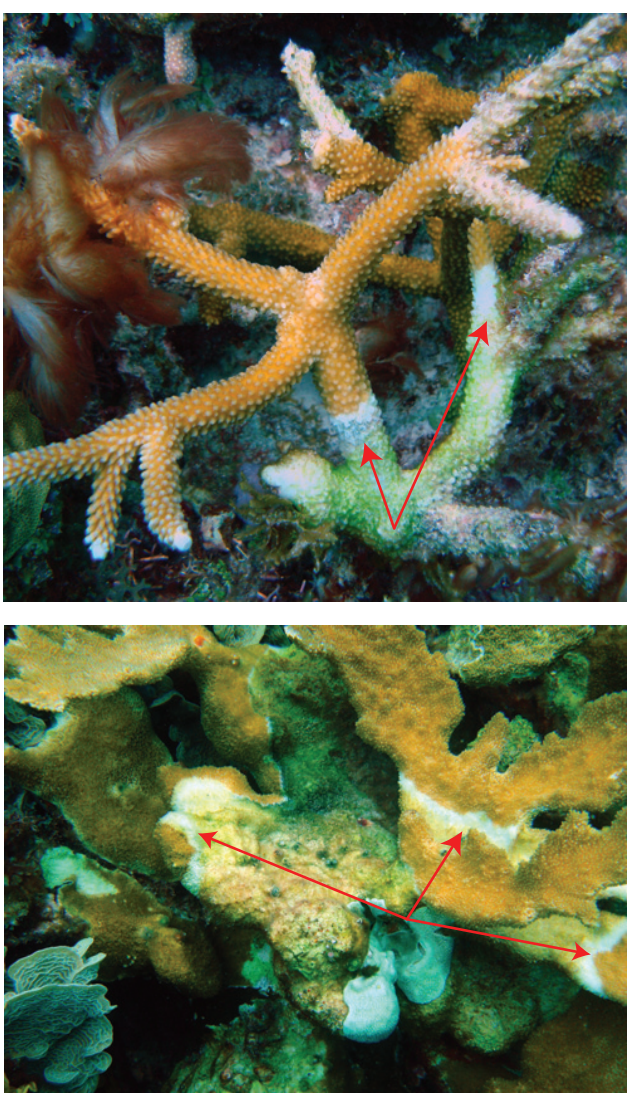

Figure 1 | Caribbean white-band disease on *Acropora* species. **a**, White-band disease on *A. cervicornis*. **b**, White-band disease on *A. palmata*. Both photos **a** and **b** were taken in Puerto Morelos, Mexico. Red arrows indicate the white bands on each colony. Photograph in **a** courtesy of A. G. Jordán-Garza.

Department of Biological Sciences, Florida Institute of Technology, 150 West University Boulevard, Melbourne, Florida 32901, USA.
*e-mail: crandall2012@my.fit.edu

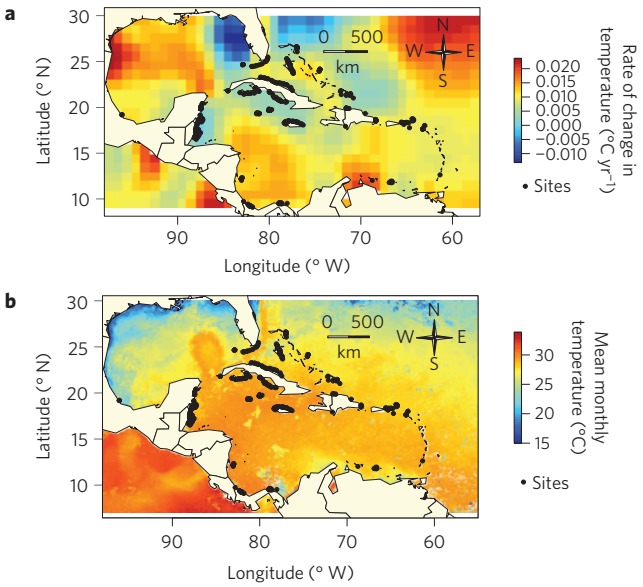

Figure 2 | Caribbean SSTs. a, Rate of change in mean monthly SSTs from 1967 to 2004 (thirty-year history before the first survey in 1997, through to the last survey in 2004) and survey-site locations. Mean monthly SSTs were obtained from the Met Office HadISST record at a spatial resolution of 1° by 1° (ref. 24). **b**, Mean monthly SST for March 1982 calculated from the Advanced Very High Resolution Radiometer (AVHRR) Pathfinder v5.2 data at a spatial resolution of 4 km by 4 km (ref. 25) and survey-site locations. Surveys were performed using the Atlantic and Gulf Rapid Reef Assessment (AGRRA) protocol.

these laboratory and field studies suggest that white-band disease is caused by one or more bacterial pathogens. Yet, the microbial communities associated with diseased-coral colonies have been inconsistent across studies[11,12]. *Acropora* colonies host microbial communities in their surface mucopolysaccharide layer, tissue layers, organic matrix and skeleton[15], and *Vibrio* spp., among other microbes, have been found in apparently healthy tissues of *A. cervicornis*[11]. It is therefore possible that white-band disease is the result of infection by microbes that already exist on corals. Several studies have hypothesized that these innate microbes may become problematic for the coral host under anomalously stressful environmental conditions[16,17]. In other words, the putative microbes may be non-pathogenic and innocuous under benign environmental conditions, but once an environmental threshold is breached the virulence and the densities of the microbes may increase, causing them to become pathogenic[15–17]. It is also plausible that white-band disease is caused by a primary-infectious pathogen that infects only corals with suppressed immune systems. The breach of temperature thresholds, as a result of warming sea surface temperatures (SSTs), has been implicated as a driver of several coral diseases[4,5,18], yet no studies have directly linked elevated SST with white-band disease in Caribbean corals.

This study examined the relationship between ocean warming and recent outbreaks of white-band disease on acroporid corals in the Caribbean. We obtained data on eight metrics that were related to historical and contemporary dynamics of SST, including 30-year rates of change in SST, thermal anomalies and thermal maxima (Table 1 and Supplementary Fig. 2). We then compared those data with the earliest comprehensive records of white-band disease on colonies of *A. palmata* and *A. cervicornis* from 473 sites across the Caribbean, from 1997 to 2004, collected by the Atlantic and Gulf Rapid Reef Assessment Program (AGRRA; Fig. 2). We also compared the disease records with habitat type and depth; based on the primary habitat of *Acropora* we restricted the analysis to sites from 0 to 15 m (Table 1). Boosted-regression-tree analyses were used to predict the response of white-band disease to each metric (Table 1), using presence and absence data.

We found that, for both species, our models performed well, achieving receiver operating characteristic (ROC) scores of 0.85 and 0.72, for *A. palmata* and *A. cervicornis*, respectively (Table 2). Most striking was that the progressive increase in seawater temperatures over the past three decades (Fig. 2a) seems to have played a significant role in the proliferation of white-band disease on the reef-building coral *A. palmata* (Fig. 3a). The models predicted a high

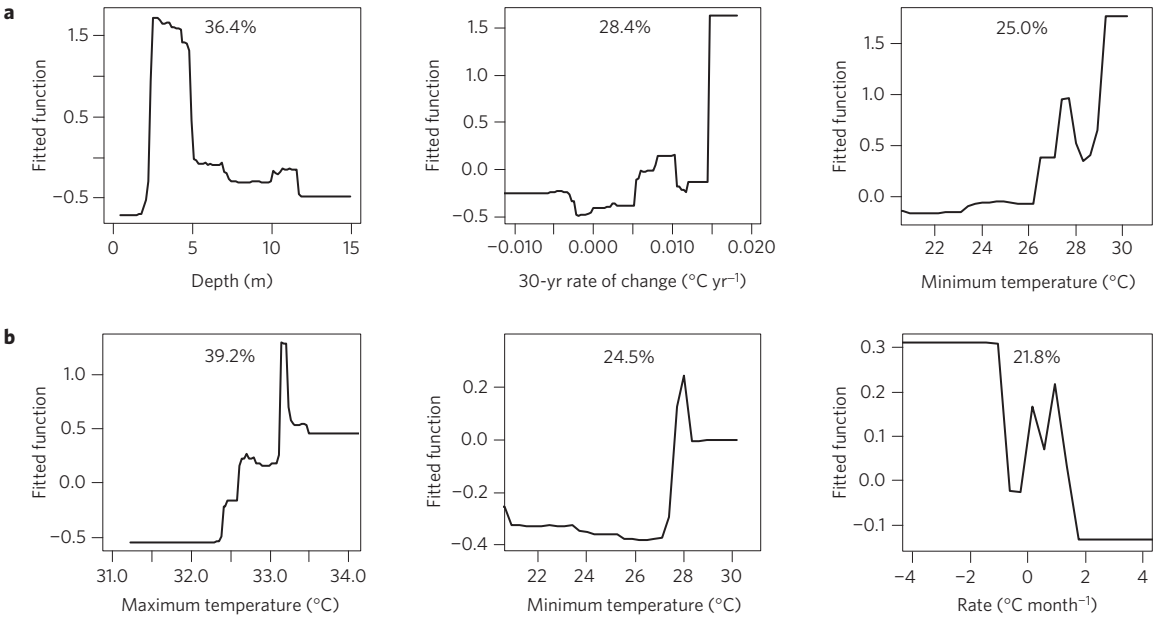

Figure 3 | Partial dependency plots. a,**b**, Partial dependency plots for the three most influential predictors (>85%) of the presence of white-band disease on *A. palmata* (**a**) and the presence of white-band disease on *A. cervicornis* (**b**), as determined from boosted-regression-tree models. Partial dependency plots are ordered based on their relative contribution to each model, and the relative importance of each predictor variable (%) is shown in each plot.

Table 1 | Definitions and relative contributions (%) of variables tested as predictors of white-band disease on *A. palmata* and on *A. cervicornis* in boosted-regression-tree models.

Predictor variables	Description	*A. palmata* presence model Relative contribution (%)	*A. cervicornis* presence model Relative contribution (%)
Minimum temperature	Minimum monthly mean SST for the 12 months before survey (°C).	25.0	24.5
Maximum temperature	Maximum monthly mean SST for the 12 months before survey (°C).	10.2	39.2
Survey temperature	Mean SST for the month and year of survey (°C).	n/a*	n/a*
Prior-month temperature	Mean SST for the month before survey (°C).	n/a*	n/a*
Survey-temperature anomaly	Mean SST anomaly for the month of survey, calculated from the 10-year monthly means (°C).	n/a*	14.5
Rate of change in temperature	Mean SST for the month before survey subtracted from the mean SST during the month of survey (°C).	n/a*	21.8
6-month cumulative anomaly	Sum of the monthly SST anomalies for the 6 months before survey, calculated from the 10-year monthly SST means (°C).	n/a*	n/a*
30-year rate of change in temperature	Rate of change in mean monthly SST for the 30 years preceding survey (°C).	28.4	n/a*
Depth	Maximum depth of survey site (m).	36.4	n/a*
Reef habitat	Categorical; Bank reef, reef crest, forereef, leeward reef, patch reef, or rhomboid reef (as per the AGRRA protocol).	n/a*	n/a*

*n/a indicates a variable that was removed from the final model, either in the simplification process, or because it was highly correlated with other predictor variables (Supplementary Table 1).

Table 2 | Model statistics for the final boosted-regression-tree models that were used to predict the presence of white-band disease on *A. palmata* and on *A. cervicornis*.

Species	# Trees	Mean total deviance	Mean residual deviance	Estimated c.v. deviance	c.v. correlation	c.v. ROC score
A. palmata	2,900	0.715	0.243	0.511 ± 0.03	0.533 ± 0.05	0.848 ± 0.02
A. cervicornis	1,400	0.594	0.375	0.539 ± 0.03	0.256 ± 0.10	0.722 ± 0.07

Models were run using a 75% bag fraction and a 10-fold cross-validation (c.v.). ROC = receiver operating characteristics curve. Values are ± standard error.

certainty of white-band disease, at any given site, when the 30-year rate of change in SST was higher than 0.015 °C yr^{-1} (Fig. 3a). This rate of increase is equivalent to an absolute temperature increase of less than half a degree Celsius over the past 30 years. In addition, there were clear temperature thresholds, both for minimum and maximum temperatures, beyond which white-band disease on both *Acropora* species seemed to proliferate (Fig. 3).

The most useful predictors of white-band disease on *A. palmata* were depth, the 30-year rate of change in temperature, and the thermal minimum the year before survey (Fig. 3a). Neither the survey temperature nor the prior-month temperature significantly contributed to predicting white-band disease on *A. palmata* (Table 1). White-band disease was most frequently recorded on *A. palmata* colonies found at a depth of 2–5 m (Fig. 3a), even though surveys encompassed a depth of 0–15 m, and there were many colonies on the shallow reef crest, between 0 and 2 m (Supplementary Fig. 3). We hypothesize that the shallowest (0–2 m) coral colonies may have had fewer cases of white-band disease than deeper (>2 m) colonies because they were locally acclimated to persistently high SST and high light, which may have consequently reduced their susceptibility to disease[19]. It is also possible that the shallow, high-energy habitats reduced thermal stress through high rates of mass transfer[20], or that high light impeded the survival and growth of putative microbial pathogens in the shallow habitat.

The long-term rate of change in temperature was the second-strongest predictor of white-band disease on *A. palmata*, and the results clearly indicated a 0.015 °C yr^{-1} threshold beyond which white-band disease increased considerably (Fig. 3a). This result suggests that white-band disease has been most prolific on colonies in localities where the rates of climate-change-driven increases in temperature have been high, whereas colonies in localities where the rates of change in temperature have been

comparatively low were less likely to experience white-band disease. The third-strongest predictor of white-band disease on *A. palmata* was the minimum temperature in the 12 months before survey (Fig. 3a). When the minimum temperature was greater than 28.5 °C, the presence of white-band disease on *A. palmata* increased. This threshold response is consistent with the hypothesis that warmer winters have the potential to relax over-wintering dormancy of pathogens, allowing infections to remain active throughout the year[21]. It is also possible that cooler winters provide seasonal relief from persistently high water temperatures to allow recovery from thermal stress. Relief and recovery are impeded however, when winters are unseasonably warm, which could weaken the corals' immune systems, potentially increasing coral susceptibility to disease.

The most useful predictors of white-band disease on *A. cervicornis* were the maximum and minimum temperatures in the 12 months before survey, and the rate of change in temperature the month preceding each survey (Fig. 3b). White-band disease on *A. cervicornis* was most evident in localities where the maximum seasonal SST exceeded a threshold of 33 °C (Fig. 3b). This result is consistent with several previous studies[4,5]. For example, a previous study on the Great Barrier Reef[4] identified a significant correlation between the frequency of white syndrome and four metrics of contemporary SST anomalies, including weekly, local, and regional thermal anomalies. Similarly, a global meta-analysis[5] identified a significant correlation between the prevalence of a suite of coral diseases and warm-temperature anomalies. The present results suggest that an acute thermal stress for a single month, above a 33 °C maximum threshold, may also severely compromise the health of *A. cervicornis*.

A. cervicornis also exhibited a threshold response to minimum temperature, showing that the presence of white-band disease on colonies increased when the minimum temperature was greater than 27.5 °C during the year before survey (Fig. 3b). Notably the results show that the threshold minimum temperature for *A. cervicornis* was one degree Celsius lower than for *A. palmata*. Therefore, *A. cervicornis*, which is more thermally sensitive than *A. palmata*, may require a lower winter minimum to recover from seasonal thermal stress. We note that the minimum-temperature threshold was revealed only when we used the high spatial resolution (4 km by 4 km) data for temperature (see the coarse-grained HadISST data analysis in the Supplementary Information). Furthermore, the long-term rate of increase in temperature was a significant predictor of white-band disease on *A. palmata*, but not on *A. cervicornis*. This long-term rate of change in temperature may play a larger role in a species, such as *A. palmata*, that is more tolerant to temperature anomalies than *A. cervicornis*. As temperatures increase over time, vulnerability thresholds may be gradually breached for *A. palmata*, resulting in bleaching and disease. By contrast, long-term temperature signals may be lost temporarily on *A. cervicornis*, which has a lower temperature threshold and experiences higher rates of mortality.

The disease on *A. cervicornis* was also predicted by the rate of change in SST the month preceding each survey (Fig. 3b); white-band disease was most common when the rate of change was negative (a 1–4 °C decrease from the previous month). In combination, these results indicate that white-band disease was most prevalent 1–2 months after the peak seasonal SST, when the temperature was declining, especially in years that had experienced considerably high thermal maxima. These results are consistent with studies that show that coral-disease outbreaks occur after coral-bleaching events and after peak summer SST (ref. 18). The present results are also consistent with the hypothesis that rapid rates of change in SST do not provide corals adequate time for thermal acclimatization, and may consequently lead to increased stress and susceptibility to disease.

The earliest aetiological studies of white-band disease stem back to the late 1970s (refs 3,22), and the most disease-susceptible coral colonies might have been already purged from both of the Caribbean acroporid populations by the time the surveys were initiated in 1997. Therefore, our analysis does not preclude the possibility that contemporary and historical white-band disease have different aetiologies. Nevertheless, these results clearly suggest that Caribbean acroporid populations are still being influenced by thermal stress associated with climate change, which is probably impeding population recovery.

Global models predict a mean increase in SST of 0.027 °C yr^{-1} from 1990 to 2090 (ref. 23), which is almost double the rate (0.015 °C yr^{-1}) that resulted in increased white-band disease on *A. palmata* reported in the present study. As SSTs continue to increase, more Caribbean localities are likely to breach the rate of change (0.015 °C yr^{-1}) and maximum temperature (33 °C) thresholds reported in the present study, resulting in white-band disease where *Acropora* populations remain. In conclusion, results from the present study suggest that both long-term climate-driven changes in SSTs, and more immediate thermal maxima, have played a significant role in the proliferation of contemporary white-band disease, and in the decline of these critically important reef-building corals in the Caribbean. We suggest that the mitigation of greenhouse gas emissions should be considered a significant component of any *Acropora*-recovery plan.

Methods

Coral-disease data. Records from 1997 to 2004 of the presence and absence of white-band disease on colonies of *A. palmata* and *A. cervicornis* (Fig. 1) were obtained from the Atlantic and Gulf Rapid Reef Assessment (AGRRA) survey program (http://www.agrra.org). To maintain consistency across survey years, data only for coral colonies ≥25 cm were included in the analyses. We also limited the depth range to 0–15 m, which is the primary habitat for both *Acropora* species. *Acropora* spp. colonies were recorded at a total of 473 sites (Fig. 2); *A. palmata* colonies were recorded at 228 sites and *A. cervicornis* colonies were recorded at 322 sites. Each survey site consisted of replicated 10 m by 1 m belt transects. Any site where a coral colony was positively identified as having white-band disease was marked as a 'present' site, and any site where no white-band disease was recorded was marked as an 'absent' site. The number of transects surveyed at each site ranged from 2 to 28 (with an average of 9 transects surveyed per site).

Temperature data. Mean monthly SST records, at a 1° by 1° spatial resolution, were obtained from the Met Office HadISST records[24]. HadISST records were used to calculate a 30-year climatology for every survey (Fig. 2a). Advanced Very High Resolution Radiometer (AVHRR) Pathfinder 5.2 (PFV5.2) nightly SST records were obtained from the National Oceanographic Data Center and GHRSST (http://pathfinder.nodc.noaa.gov)[25], and monthly averages were calculated for 1982–2012, at a 4 km by 4 km spatial resolution (Fig. 2b). Pathfinder records were used to calculate all temperature predictors except for the 30-year climatology, which required the long-term (HadISST) data set. We tested eight metrics, which were related to the dynamics of SST, as potential predictors of white-band disease (see Supplementary Methods for temperature metric definitions; Table 1 and Supplementary Fig. 2). Pair-wise Pearson's correlation coefficients were evaluated to determine which, if any, predictor variables were collinear (Supplementary Table 1). To avoid issues of collinearity, we conservatively discarded any environmental predictor variables whose statistically significant correlation coefficients were >0.5 with a co-occurring predictor, despite the capacity of the boosted-regression-tree-modelling technique to differentiate potentially correlated predictors[26] (Supplementary Table 1).

We included only one survey site per grid cell, during any given month and year, for the analysis using the 4 km by 4 km Pathfinder data. If any survey within an individual grid cell recorded white-band disease, the disease was considered present within that grid cell. This resulted in a total of 182 records of *A. palmata* and 251 records of *A. cervicornis* being included in the models. For the 30-year climatology, there were a total of 182 records of *A. palmata* within 65 (100 km by 100 km) grid cells, and 251 records of *A. cervicornis* within 72 grid cells (3.5 ± 2.6 surveys per grid cell for *A. palmata* and 4.5 ± 3.7 surveys per grid cell for *A. cervicornis*). Given the heterogeneous nature of reefs at the 100 km by 100 km spatial scale, the use of 3–5 survey sites within a single grid cell seems reasonable for climatological records. For comparison with the fine scale (4 km by 4 km) temperature data, a second set of boosted-regression-tree models

was run using temperature predictors calculated from the coarse-grained HadISST data set (100 km by 100 km). These results are presented in the online Supplementary Information (Supplementary Table 2 and Supplementary Fig. 4).

Model. The boosted-regression-tree technique combines regression trees and boosting, by iteratively fitting new trees to a model that best reduces the model's deviance. More formally, a boosted-regression-tree model is an additive regression model that takes the form:

$$f(x) = \sum_{m=1}^{n} \beta_m b(x; \gamma_m)$$

where β_m is a vector of weighted constants for each node of the tree, x is the predictive variable, and γ_m is a matrix that defines the splitting variables, their values at each node, and the predicted values; the function $b(x; \gamma_m)$, therefore, represents the 'tree'[27]. Trees are constructed recursively and added to the model sequentially from m to n, and each subsequent tree is added to minimize the loss function of the model. The loss function is defined as:

$$L(y, f(x)) = [r - \beta b(x; \gamma)]^2$$

where r is the least-squares residuals[27]. Stochasticity is incorporated into the model by bagging, which uses a bootstrapped subset of data (here we used 75%, with replacement) to fit each new tree. This probabilistic component, combined with a model-simplification procedure, reduces overfitting and improves the model's accuracy[27,28]. In the present study, the boosted-regression-tree model was constructed using the package *'gbm'* version 2.1 (ref. 29), and using code written by Elith *et al.*[28], in the R statistical program[30]. A k-fold cross-validation procedure was used to train (90%) and test (10%) each model. The relative contribution of each predictor variable was estimated[28], and any interactions between predictor variables were examined[29].

Received 27 October 2014; accepted 11 January 2015; published online 16 February 2015

References

1. Aronson, R. B. & Precht, W. F. White-band disease and the changing face of Caribbean coral reefs. *Hydrobiologia* **460,** 25–38 (2001).
2. Pandolfi, J. Coral community dynamics at multiple scales. *Coral Reefs* **21,** 13–23 (2002).
3. Antonius, A. *Proc 4th Int. Coral Reef Symp.* Vol. 2, 7–14 (Marine Sciences Center, University of the Philippines, 1981).
4. Selig, E. R. *et al. Coral Reefs and Climate Change: Science and Management* 111–128 (American Geophysical Union, 2006).
5. Ruiz-Moreno, D. *et al.* Global coral disease prevalence associated with sea temperature anomalies and local factors. *Dis. Aquat. Organ.* **100,** 249–261 (2012).
6. Budd, A. F., Stemann, T. A. & Stewart, R. H. Eocene Caribbean reef corals: A unique fauna from the Gatuncillo Formation of Panama. *J. Paleontol.* **66(4),** 570–594 (1992).
7. Zachos, J. C., Dickens, G. R. & Zeebe, R. E. An early Cenozoic perspective on greenhouse warming and carbon-cycle dynamics. *Nature* **451,** 279–283 (2008).
8. Aronson, R., Bruckner, A., Moore, J., Precht, B. & Weil, E. *Acropora palmata The IUCN Red List of Threatened Species* 2014.2. (International Union for Conservation of Nature and Natural Resources, 2008); http://www.iucnredlist.org
9. Hogarth, W. T. Endangered and threatened species: Final listing determinations for elkhorn and staghorn coral. *Fed. Reg.* **71,** 26852–26861 (2006).
10. Randall, C. J., Jordan-Garza, A. G., Muller, E. & vanWoesik, R. Relationships between the history of thermal stress and the relative risk of Caribbean corals. *Ecology* **95,** 1981–1994 (2014).
11. Ritchie, K. B. & Smith, G. W. Type II white-band disease. *Rev. Biol. Trop.* **46,** 199–203 (1998).
12. Pantos, O. & Bythell, J. C. Bacterial community structure associated with white band disease in the elkhorn coral *Acropora palmata* determined using culture-independent 16S rRNA techniques. *Dis. Aquat. Organ.* **69,** 79–88 (2006).
13. Sweet, M. J., Croquer, A. & Bythell, J. C. Experimental antibiotic treatment identifies potential pathogens of white band disease in the endangered Caribbean coral *Acropora cervicornis*. *Proc. R. Soc. B* **281,** 20140094 (2014).
14. Lentz, J. A., Blackburn, J. K. & Curtis, A. J. Evaluating patterns of a white-band disease (WBD) outbreak in *Acropora palmata* using spatial analysis: A comparison of transect and colony clustering. *PLoS ONE* **6,** e21830 (2011).
15. Rosenberg, E., Koren, O., Reshef, L., Efrony, R. & Zilber-Rosenberg, I. The role of microorganisms in coral health, disease and evolution. *Nature Rev. Microbiol.* **5,** 355–362 (2007).
16. Lesser, M. P., Bythell, J. C., Gates, R. D., Johnstone, R. W. & Hoegh-Guldberg, O. Are infectious diseases really killing corals? Alternative interpretations of the experimental and ecological data. *J. Exp. Mar. Biol. Ecol.* **346,** 36–44 (2007).
17. Muller, E. M. & van Woesik, R. Caribbean coral diseases: Primary transmission or secondary infection? *Glob. Change Biol.* **18,** 3529–3535 (2012).
18. Miller, J. *et al.* Coral disease following massive bleaching in 2005 causes 60% decline in coral cover on reefs in the US Virgin Islands. *Coral Reefs* **28,** 925–937 (2009).
19. Howells, E. J. *et al.* Coral thermal tolerance shaped by local adaptation of photosymbionts. *Nature Clim. Change* **2,** 116–120 (2012).
20. Nakamura, T. & vanWoesik, R. Water-flow rates and passive diffusion partially explain differential survival of corals during the 1998 bleaching event. *Mar. Ecol. Prog. Ser.* **212,** 301–304 (2001).
21. Harvell, C. D. *et al.* Climate warming and disease risk for terrestrial and marine biota. *Science* **296,** 2158–2162 (2002).
22. Gladfelter, W. B. White-band disease in *Acropora palmata*: Implications for the structure and growth of shallow reefs. *Bull. Mar. Sci.* **32,** 639–643 (1982).
23. Bopp, L. *et al.* Multiple stressors of ocean ecosystems in the 21st century: Projections with CMIP5 models. *Biogeosciences* **10,** 6225–6245 (2013).
24. Rayner, N. A. *et al.* Global analyses of sea surface temperature, sea ice, and night marine air temperature since the late nineteenth century. *J. Geophys. Res.* **108 D14,** 4407 (2003).
25. Casey, K. S., Brandon, T. B., Cornillon, P. & Evans, R. in *Oceanography from Space: Revisited* (eds Barale, V., Gower, J. F. R. & Alberotanza, L.) 323–341 (Springer, 2010).
26. Dormann, C. F. *et al.* Collinearity: A review of methods to deal with it and a simulation study evaluating their performance. *Ecography* **36,** 027–046 (2013).
27. De'ath, G. Boosted trees for ecological modeling and prediction. *Ecology* **88,** 243–251 (2007).
28. Elith, J., Leathwick, J. R. & Hastie, T. A working guide to boosted regression trees. *J. Animal Ecol.* **77,** 802–813 (2008).
29. Ridgeway, G. *Generalized Boosted Regression Models Version. 1. Doc. R Package 'gbm'* Vol. 7 (R Foundation for Statistical Computing, 2006); http://cran.fiocruz.br/web/packages/gbm/gbm.pdf
30. R Core Team, *R: A Language and Environment for Statistical Computing* (R Foundation for Statistical Computing, 2014); http://www.R-project.org

Acknowledgements

We thank the Atlantic and Gulf Rapid Reef Assessment Program for training volunteers, conducting surveys, and making data freely available for use, especially R. Ginsburg, J. Lang and P. Kramer. Thanks also to S. J. van Woesik and J. E. Speaks for editorial comments, to C. Cacciapaglia for assistance with coding, to R. Aronson for valuable discussions, and to A. G. Jordán-Garza for providing a photograph of *A. cervicornis*. We acknowledge NSF OCE-1219804, awarded to R.v.W., for funding. This paper is Contribution No. 126 from the Institute for Research on Global Climate Change at the Florida Institute of Technology.

Author contributions

C.J.R. and R.v.W. conceived and designed the experiments; C.J.R. performed the experiments, coded the models and analysed the data; both authors wrote the manuscript.

Additional information

Supplementary information is available in the online version of the paper. Reprints and permissions information is available online at www.nature.com/reprints. Correspondence and requests for materials should be addressed to C.J.R.

Competing financial interests

The authors declare no competing financial interests.